Biodegradation **2**: 171–179, 1992.

Biological fate of a polydisperse acrylate polymer in anaerobic sand-medium transport

Bruce E. Rittmann,[1] Benjamin Henry,[2] Joseph E. Odencrantz[3] & Julie A. Sutfin[4]
[1] *Environmental Engineering and Science, University of Illinois at Urbana-Champaign, 205 North Mathews Avenue, Urbana, IL 61801, USA;* [2] *County Sanitation Districts of Los Angeles County, 1955 Workman Mill Road, Whittier, CA 90607, USA;* [3] *Levine-Fricke Engineers, 1920 Main Street, Suite 750, Irvine, CA 92714, USA;* [4] *John Mathes & Assoc., Inc., 210 West Sand Bank Road, Columbia, IL 62236, USA*

Received 23 September 1991; accepted in revised form 15 January 1992

Key words: acrylate, adsorption, biodegradation, biotic fate, contact time, methanogenic consortium, modeling, polyacrylate, polydisperse, retardation

Abstract

Soluble polyacrylate (PA), a polydisperse mixture of polyacrylate polymers, is strongly adsorbed and biodegradable. Biotic fate studies were carried out with once-through columns containing sand colonized with anaerobic biomass previously grown in a methanogenic fluidized bed. A fraction of soluble PA having a weight-average molecular weight of 16,700 and a range of molecular weight from 10^3 to 10^5 was biologically removed and mineralized to CO_2. Due to its polydisperse nature, the breakthrough curve had a gradual increase to an apparent steady-state removal of approximately 60% near one day when the liquid detention time was 21 minutes. Modeling successfully explained the observed breakthrough result when the fraction was divided into components having a wide range of retardation factors (R): about 25% was strongly adsorbed (R = 200 and 500), 45% was moderately adsorbed (R = 50 and 100), and 30% was weakly adsorbed (R = 1–10). In this study, in which active biomass already was present from utilization of a primary substrate (glucose here), equilibrium adsorption increased the time to breakthrough, which also reduced the exiting concentration by increasing the substrate contact time.

Introduction

In our previous report (Rittmann et al. 1992), we showed three things about a fraction of soluble PA (polyacrylate) made of polymerized acrylate:

1. It was highly polydisperse, having a weight-averaged molecular weight (M_w) of 16,700 and a range of molecular weight from 10^3 to 10^5.
2. Although about 1% was unabsorbed by sand, the remaining soluble PA was strongly adsorbed, having an average retardation factor of at least 58.
3. Although its biodegradation kinetics were slow compared to glucose and acrylate, the soluble PA was removed and partially mineralized to CO_2 by a methanogenic biofilm community.

This report describes the interactions among these three factors when soluble PA is transported through a porous medium that has an active microbial population. This situation represents the phenomena that could occur if soluble PA were to leach from a landfill. First, the background organic material can support growth of anaerobic biofilm on the surfaces of the soil particles. Second, adsorption to the soil particles and to the biomass can retard the transport of most of the PA and reduce

its liquid-phase concentration. Finally, the biomass can biodegrade the polymers.

The most important interaction is the one between adsorption and biodegradation. Does adsorption increase or decrease the amount of soluble PA that is biodegraded? On the one hand, retardation increases the time that the substrate is in the biologically active zone. One the other hand, the liquid-phase concentration is decreased by adsorption, which is a competing sink to biodegradation. Chang and Rittmann (1988) demonstrated by experiment and modeling that adsorption to granular activated carbon (GAC) slowed the onset of biodegradation when two factors were acting: (1) the adsorption was in micropores that were not accessible to the bacteria, and (2) the biofilm grew from a small inoculum solely through utilization of the adsorbable substrate. When the biofilm population became large, Chang and Rittmann (1988) found no effect of adsorption, because the substrate utilization was fast and out-competed adsorption. The situation of soluble PA in a groundwater environment is different from that of Chang and Rittmann (1988), because (1) the adsorbed substrate is not in micropores (the sand has very limited micropores) and is adsorbed relatively close to the microorganisms, and (2) the biomass need not be grown only through utilization of the soluble AGM, since other biodegradable organic material is present to serve as a primary substrate (Kobayashi & Rittmann 1982). Thus, adsorption may enhance biodegradation, if the positive effects of increased contact time out-weigh the negative effects of a lower liquid phase concentration.

For soluble PA, the situation is further complicated by its polydisperse nature. While some portion of the material has little or no retardation, the majority of the material is strongly adsorbed. The large range of molecular weights (Rittmann et al. 1992) suggests that the adsorbed materials exhibit a wide range of retardation factors.

In this report, we document the simultaneous biodegradation and adsorption of soluble PA as it is transported through a sand column that has attached anaerobic biomass. We evaluate the hypothesis that the complex breakthrough response is controlled by a range of retardation factors characteristic of the polydisperse material.

Materials and methods

Substrates

The substrates were glucose, acrylate, and a fraction of soluble PA produced by fractional precipitation and denoted by its weight-averaged molecular weight, M_w 16,700. Details on the ^{14}C-labelled and unlabelled substrates are found in Rittmann et al. (1992).

Fluidized-bed biofilm reactor

In order to generate sand with a uniform and nonclogging accumulation of biofilm, we operated the fluidized-bed system illustrated in Fig. 1. The tubular reactor was glass with an inside diameter of 2.5 cm and a total length of 92 cm. A recycle outlet was located 8 cm from the top, and a port for sand removal was located 8 cm from the bottom. The teflon end caps had a conical interior. A teflon screen was placed on top of the bottom cap, followed by 2 cm of 0.3-cm glass beads and 2 cm of 0.1-cm glass beads for flow distribution. The recycle components consisted of Tygon tubing, a heater tank (35 ± 1 °C), and two peristaltic pumps in parallel. The two parallel pumps were needed to ensure bed fluidization at all times, including when the tubing was replaced (weekly) for one pump. The medium was the seived Borden sand described in Rittmann et al. (1992). The reactor and heater tank were covered with aluminum foil to exclude light.

The feed solution was supplied by a peristaltic pump and entered the system in the recycle line. The composition of the feed solution is given in Table 1. Glucose was the primary substrate for supporting the mixed methanogenic consortium. The pH was buffered to 7.0 ± 0.1 by the phosphate and bicarbonate salts. The sterile and deoxygenated feed solution was prepared by the procedures given by Rittmann et al. (1992).

The fluidized bed was seeded with an inoculum from another methanogenic biofilm reactor in the laboratory. After inoculation, the feed rate was set at 0.2 ml/min and gradually increased to 1 ml/min over a 2-week period. After 3 months of continuous operation with the 1 ml/min flow rate, analysis of the gas composition using a gas partitioner (Fisher Gas Chromatograph Model 1200) showed formation of CO_2 and CH_4. Furthermore, sand stained with crystal violet demonstrated that bacteria had colonized the crevices of the sand (Henry 1990). The high shear forces in the fluidized bed prevented growth on the exposed areas of the sand. Table 2 summarizes operating conditions for the fluidized-bed reactor.

Biotic fate experiments

The fates of acrylate and fraction M_w 16,700 in biologically active sand were determined in once-through tracer tests. The experimental set-up was the same as used by Rittmann et al. (1992). Two differences in the experimental protocol were required. First, colonized sand was transferred from the fluidized bed to the once-through packed bed. The packed-bed column was filled with de-oxygenated medium (the first 11 ingredients in Table 1). Then, the packed-bed column was placed under the sand-removal port of the fluidized bed. The effluent valve was closed, and the sand-removal port was opened. The feed rate to the fluidized bed was increased to 10 ml/min, which forced sand/

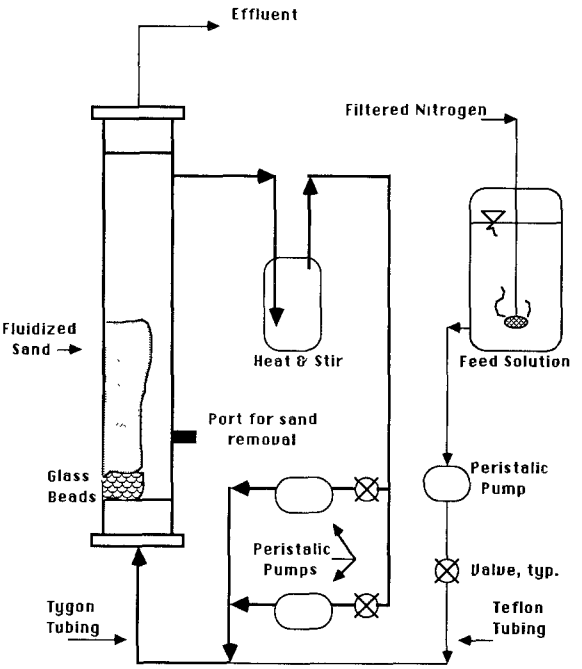

Fig. 1. Schematic of the fluidized-bed system used for biofilm development.

Table 1. Composition of the feed solution to the anaerobic fluidized-bed reactor.

Component	Concentration (mg/l)
NH_4Cl	145
KH_2PO_4	855
K_2HPO_4	648
$NaHCO_3$	84
$CaCl_2$	2
$MnCl_2 \cdot 4H_2O$	0.2
$MgCl_2 \cdot 6H_2O$	16.9
$NaMoO_4 \cdot 2H_2O$	0.1
$FeCl_2 \cdot 4H_2O$	6.25×10^{-3}
$Na_2S \cdot 9H_2O$	30
Resazurin	0.9
Glucose	100
Vitamin solution	1.25 ml/l
d-Biotin	2
Folic acid	2
Pyridoxin HCl	10
Riboflavin	5
Thiamine	5
Nicotinic acid	5
D-Pantothenic acid	5
Vitamin B_12	0.1
P-Amino benzoic acid	5
Thioctic acid	5

Table 2. Operating conditions for the fluidized-bed reactor.

Total length of column	92 cm
Diameter of column	2.5 cm
Volume of sand (unexpanded)	150 cm^3
Surface area of sand	192 m^2
Feed flow rate, Q	1 ml/min.
Recycle flow rate, Q_R	200 ml/min.
Surface loading	0.8 mg as COD/m^2-day
Influent substrate concentration	107 mg as COD/l
Diameter of sand (average)	0.16 mm
Temperature	21 ± 2 °C

water slurry into the packed column. As the column filled with sand, it was gently tapped to evenly distribute and pack the bed. When the bed was fully packed, the top end cap was put in place, the effluent tubing was connected, and anaerobic mineral medium (Table 1, but with no substrate) was pumped through at 1 ml/min for approximately 30 minutes. The second difference involved the duration of the experiments. After 30 minutes, the anaerobic mineral medium with appropriate substrate (glucose, acrylate, or fraction M_w 16,700) was fed at a flow rate of 0.25 ml/min, giving a liquid detention time of 21.2 minutes. Substrate feeding from a reservoir was continuous for up to three days. The total concentration (as C) was controlled by adding unlabelled substrate, while a small mass of ^{14}C substrate was added for assay by scintillation counting.

Sampling and analytical methods

Influent and effluent samples were collected in 5-ml ground-glass syringes that had been blocked with unlabelled substrate (Rittmann et al. 1992). The ^{14}C concentrations of soluble organic carbon, CO_2, and suspended biomass were measured by the sample treatments and scintillation counting described by Rittmann et al. (1992).

Modeling

The results of the biotic fate experiments were modeled with a finite-element computer model that coupled one-dimensional solute transport, adsorption, and biofilm degradation kinetics. The basic mass-balance equation is the advection-dispersion equation with equilibrium adsorption and biofilm reaction (Freeze and Cherry 1979; Odencrantz et al. 1990, 1991):

$$D_H \frac{\partial^2 C}{\partial x^2} - U\frac{\partial C}{\partial x} - K_p \frac{\varrho_b}{\varepsilon}\frac{\partial C}{\partial t} - aJ = \frac{\partial C}{\partial t} \quad (1)$$

in which

C = solute concentration [ML^{-3}]
x = distance dimension along the flow path [L]
t = time [T]
D_H = hydrodynamic dispersion coefficient [L^2T^{-1}]
U = one-dimensional interstitial flow velocity [LT^{-1}]
K_p = equilibrium partition coefficient [L^3M^{-1}]
ϱ_b = bulk density of the aquifer solids [ML^{-3}]
ε = porosity
a = specific surface area of biofilm colonization [L^{-1}]
J = substrate flux into the biofilm [$ML^{-2}T^{-1}$]

The retardation factor, R, is defined as

$$R = 1 + K_p \frac{\varrho_b}{\varepsilon} \quad (2)$$

and represents the relative retention time of the adsorbed solute compared to the water (in the absence of biodegradation). Thus, Eq. 1 can be rewritten as

$$D_H \frac{\partial^2 C}{\partial x^2} - U\frac{\partial C}{\partial x} - aJ = R\frac{\partial C}{\partial t} \quad (3)$$

Equation 3 was solved numerically by the method of operator splitting, which solves the equation in two steps (Wheeler 1988; Wheeler & Dawson 1987). In the first step, only the nonreactive terms,

$$D_H \frac{\partial^2 C}{\partial x^2} - U\frac{\partial C}{\partial x} = R\frac{\partial C}{\partial t} \quad (4)$$

were solved by the Principle Direction Finite Element Method (PDFEM) of McQuarrie et al. (1989). Then, the reactive portion,

$$-aJ = R\frac{\partial C}{\partial t} \quad (5)$$

was solved by a fourth-order Runge-Kutta ordinary differential equation solver with initial conditions taken from the PDFEM solution of Eq. 4.

The biofilm flux in Eq. 5 was computed by the algorithm of Rittmann and McCarty (1981). The algorithm computes J according to

$$J = \eta\, X_f L_f\, q_{max} \frac{C_s}{K + C_s} \qquad (6)$$

in which

- η = an effectiveness factor that describes the effects of substrate diffusion within the biofilm
- X_f = biofilm density [ML^{-3}]
- L_f = biofilm thickness [L]
- q_{max} = maximum specific rate of substrate utilization [$MM^{-1}T^{-1}$]
- K = half-maximum-rate concentration [ML^{-3}]
- C_s = substrate concentration at the biofilm/liquid interface [ML^{-3}]

Equation 6 is subject to a boundary condition that represents mass-transport resistance at the biofilm/liquid interface:

$$J = \frac{D}{L}(C - C_s) \qquad (7)$$

in which

- D = molecular diffusion coefficient for the substrate [L^2T^{-1}]
- L = thickness of an effective diffusion layer [L].

The algorithm of Rittmann and McCarty solves Eq. 6 for J, subject to the boundary condition Eq. 7 and a set of equations defining η in terms of L_f, C_s, and the substrate's diffusion coefficient in the biofilm, D_f [L^2T^{-1}]. The inputs to the algorithm are C, X_f, L_f, q_{max}, K, D, L, and D_f.

The biodegradation kinetic parameters (q_{max}, K) and diffusion parameters (D, D_f) were estimated by Rittmann et al. (1992) for acrylate and fraction M_w 16,700. The flow velocity was controlled for each experiment. The values of L was estimated for each velocity from the equations given by Rittmann et al. (1992). D_H was computed to be 82 cm^2 per day from the results of a pulse-input tracer study using acrylate (Henry 1990; Levenspiel 1972) as the conservative tracer. The total biomass (X_fL_fa) was calibrated from experimental results with acrylate, as described below.

For fraction M_w 16,700, breakthrough curves were generated for a range of retardation factors: R = 1, 2, 5, 10, 50, 100, 200, and 500. These curves were then combined to give a best-fit composite curve that represented the polydisperse nature of the soluble AGM. The means of generating a composite curve assumed that the same kinetic parameters described biodegradation for all retardation factors. Rittmann et al. (1992) determined that changes in the mass-transport parameters did not alter the flux, because the kinetics were limited completely by the biodegradation rate.

Results and discussion

Acrylate

Acrylate experiments were carried out at four different combinations of flow rate and background glucose concentration. In each case, the effluent acrylate concentration, measured as soluble organic C, quickly (< 1 hour) reached a stable plateau value indicative of steady-state. Table 3 presents the fate of the influent ^{14}C for each steady state.

Decreasing the flow rate, which proportionally increased the contact time from 5.3 to 21.2 min-

Table 3. Fate of ^{14}C in acrylate fed at 0.05 mg C/l for different glucose concentrations and flow rates.

Glucose conc. (mg/l)	Flow rate (ml/min)	Percent of influent ^{14}C in effluent			
		Total	Soluble org.	CO_2	Cells
1.0	1.0	100	83	4	13
1.0	0.5	100	52	32	16
0.1	0.5	100	51	33	16
0.1	0.25	100	12	72	16

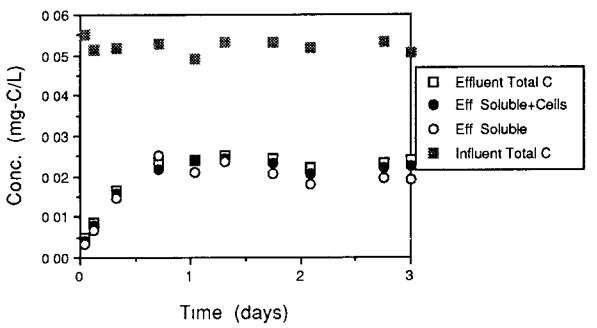

Fig. 2. Breakthrough results for the biotic fate experiment with fraction M_w 16,700 and a flow rate of 0.25 ml/min.

utes, caused the expected decrease in effluent soluble organic C and increase in CO_2 - C. The presence of glucose in the feed did not affect acrylate utilization. The 100% recovery of influent ^{14}C implies that acrylate was not fermented to CH_4. The carboxyl group on acrylate probably was oxidatively cleaved to CO_2, yielding ethene, which must have been oxidized to CO_2. Since glucose was present during each experiment, cell synthesis probably was supported almost totally by unlabelled carbon from glucose.

The one-dimensional solute-transport model was used to estimate the amount of attached biomass, $X_f L_f a$, from the acrylate results, because accurate direct measurement was impossible for the relatively low level of colonization in the sand's crevices. Acrylate was ideal for the calibration, because it does not adsorb and its utilization and transport parameters are known (Rittmann et al. 1992): q_{max} = 0.066 gC/g biomass-day, K = 0.11 g C/m^3, D = 0.57 cm^2/day, D_f = 0.46 cm^2/day, and L = 30 μm. The transport model was run for the acrylate experiments having a flow rate of 0.25 ml/min, because this run gave the most stable estimate of the effluent concentration. The three parameters –X_f, L_f, and a – were varied systematically over their feasible ranges, and the best-fit set of parameters was the one giving the experimentally observed effluent concentration (0.0051 mg C/l) and no systematic deviations. The best-fit values were: X_f = 55.35 mg biomass/cm^3, L_f = 2μm, a = 25 cm^{-1}, and $X_f L_f a$ = 0.277 mg/cm^3. The last value corresponds to 770 mg biomass/l of liquid pore volume, an expectedly low value for a biofilm reactor that should have no clogging potential. The specific surface area of 25 cm^{-1} corresponds to approximately 10% of the total surface area that could have been colonized.

Fraction M_w 16,700

Figure 2 presents the breakthrough results for fraction M_w 16,700. Five features are important. First, the breakthrough of soluble organic ^{14}C is gradual for about 0.75 day (recall that the liquid detention time is 21.2 minutes) and approaches an apparent steady state. Second, the apparent steady state has an effluent concentration of soluble organic ^{14}C equal to 37% of the influent ^{14}C. Third, the CO_2 - ^{14}C equals 2.2% of the influent ^{14}C. Fourth, the effluent cellular ^{14}C equals 5.6% of the influent ^{14}C. Finally, the total ^{14}C is 45% of the influent ^{14}C, which means 55% removal of the influent ^{14}C.

The five observations about the fate of fraction M_w 16,700 can be explained conceptually by its polydisperse nature. The strong adsorbability of much of the material explains the long and gradual breakthrough, the 55% total removal, and the 63% removal of soluble organic ^{14}C with only 2.2% production of CO_2 - ^{14}C. A superficial comparison of the results for fraction M_w 16,700 and acrylate would suggest that M_w 16,700 had almost as much biodegradation as did acrylate acid, even though the measured biodegradation kinetics of fraction M_w 16,700 were much slower than for acrylate (Rittmann et al. 1992). In reality, the biodegradation kinetics of fraction M_w 16,700 remained much slower, but retardation of the most strongly adsorbed materials of the polydisperse fraction increased its long-term removal.

The one-dimensional solute-transport model was used to describe quantitatively the interacting mechanisms of advection, dispersion, adsorption, and biodegradation. Fraction M_w 16,700 was divided into eight components having retardation factors 1, 2, 5, 10, 50, 100, 200, and 500. The biodegradation and transport parameters measured by Rittmann et al. (1992) were assumed for each component: q_{max} = 0.0016 g C/g biomass-day, K = 0.79

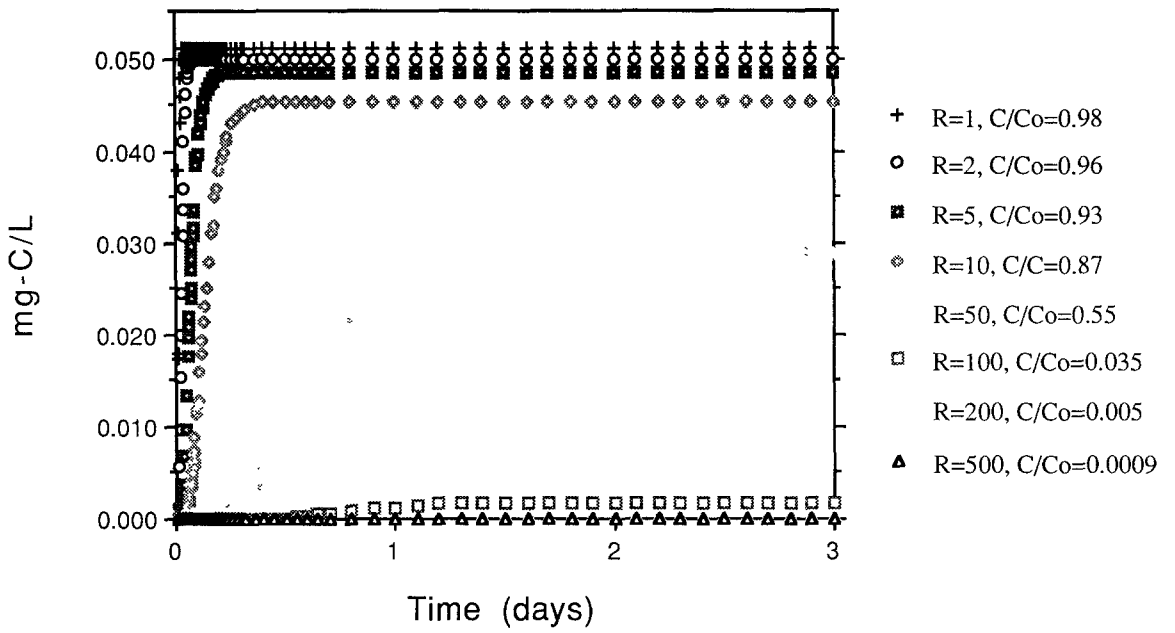

Fig. 3. Component curves for the simultaneous transport, dispersion, adsorption, and biodegradation of portions of fraction M_w 16,700 having different retardation factors. The flow rate is 0.25 ml/min. The ratio C/C_0 refers to the steady-state effluent concentration for each portion.

mg C/l, D = 0.041 cm^2/day, D_f = 0.032 cm^2/day, and L = 4.7 μm. [Due to the slow biodegradation kinetics, the result was not sensitive to choices for D, D_f, and L (Rittmann et al. 1992).] The X_f, L_f, and a values were those calibrated from acrylate.

The model was solved for each component separately for a flow rate of 0.25 ml/min, an influent concentration of 0.052 mg C/l, and a 3-day experiment. Figure 3 shows the breakthrough curves for each component. The component curves fall into 3 characteristic groupings.

- R $\leq$ 10. Breakthrough is relatively rapid, and a steady-state removal is achieved, since retardation is not great. The effluent concentration at steady state decreases as the retardation factor and the resultant contact time increase.
- R = 50 and 100. These curves show substantially delayed breakthrough, but a steady-state removal is achieved eventually (at about 3.5R times the liquid detention time). As before, the steady-state removal is greater for the larger contact time.
- R $\geq$ 200. These curves have a very delayed breakthrough and high steady-state removals. Although the scale does not illustrate it, breakthroughs had begun before 3 days, but had not reached steady state in 3 days.

The experimental response in Fig. 2 was fit by combining the component curves to create one composite curve that represented the polydisperse nature of fraction M_w 16,700. The composite curve was the weighted sum of component curves and was computed for each time step by

$$C_t = C_o \sum_{i=1}^{8} \left(\frac{C_t}{C_o}\right)_i f_i \tag{8}$$

in which C_t = the composite concentration at time t, C_o = the total influent concentration (0.052 mg C/l), $(C_t/C_o)_i$ = the ratio of C_t to C_o for component curve i at time t, and f_i = the fraction of C_o attributed to component i. Mass balance was assured by setting

$$1 = \sum_{i=1}^{8} f_i \tag{9}$$

Figure 4 presents the best-fit composite curve and the f_i values for each component. Because the composite curve was matched by a trial-and-error pro-

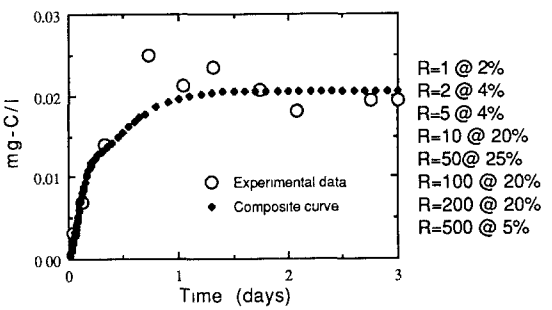

Fig. 4. Composite curve and distribution of retardation factors for fraction M_w 16,700. The legend gives the composite curve's f_i values (as a percentage) according to each retardation factor. The vertical axis gives the effluent soluble C concentration. The data corresponds to those in Fig. 2, for which the average influent soluble C is 0.052 mg C/l.

cedure, the best fit was not precisely defined statistically. Although other possibilities for the percentage distribution may be possible, the distribution given in Fig. 4 matches the trends and explains how the polydisperse nature of fraction M_w 16,700 controlled its fate.

The rapid increase in effluent concentration during the first 4 hours was controlled by the 30% of influent material having $R \leq 10$. This material broke through relatively quickly and had relatively little biodegradation. The less rapid increase from 4 hours to 1 day was controlled by the 45% of mass having a moderate R, represented by R = 50 and 100. The nearly flat response after 1 day was determined mainly by the remaining 25% of mass being strongly adsorbed (R = 200 and 500).

Figure 2 shows about 63% removal of soluble organic ^{14}C. However, the component distribution in Fig. 4 indicates that more than 30% of that removal was adsorption, retention, and biodegradation of components with R = 200 and 500. These components were not yet at steady state. If the test had been run long enough to have complete breakthrough of all components, the model predicts that the steady-state removal would have been somewhat less, near 60%. However, the increased removal of the more highly retarded compounds increased the long-term biodegradation and gave a percentage biodegradation greater than would be expected from the biodegradation kinetics alone.

Although the modeling approach used here successfully represented the experimental results and provided an intuitive explanation for the interactions between adsorption with biodegradation with a polydisperse substrate, it has limitations that should be explicitly stated. First, we assumed that all variability within fraction M_w 16,700 was explained by changes in the retardation factor, while the intrinsic biodegradation kinetics were constant. While this assumption is consistent with the data presented here and by Rittmann et al. (1992), it cannot be proven or disproven by these results. Perhaps the biodegradation kinetics also change with increasing molecular size. Second, the range of retardation factors used here is only qualitatively related to the retardation properties described in Rittmann et al. (1992). Independent determination of the distributions of retardation factors by tracer experiments is desirable, but unfeasible. Finally, the model did not include a mass balance on ^{14}C-CO_2, which would have allowed a prediction of the effect of adsorption in mineralization, which is an ultimate proof of biodegradation.

Conclusions

Biotic fate studies were carried out with once-through columns containing sand colonized with anaerobic biomass previously grown in a methanogenic fluidized bed. Acrylate was mineralized to CO_2, and the percent removal increased from 17% to 88% as the flow rate was decreased from 1 ml/min to 0.25 ml/min. 100% of the influent ^{14}C tracer was recovered as effluent soluble organic, CO_2, or cellular ^{14}C. Hence, the acrylic acid monomer was not adsorbed or fermented to CH_4. The steady-state results for acrylic acid removal were used to calibrate the biomass accumulation for a one-dimensional solute-transport model for advection, dispersion, equilibrium adsorption, and biofilm biotransformation. The amount of attached biomass was 0.277 mg biomass/cm^3 of reactor volume.

Soluble PA fraction M_w 16,7000 showed biodegradation and mineralization to CO_2, although mineralization was only 2.2% of the influent ^{14}C. Due to its polydisperse nature, the breakthrough

curve showed a gradual increase to an apparent steady-state removal of approximately 63% near one day. Modeling analysis used the biodegradation parameters measured by Rittmann et al. (1992) and a composite breakthrough curve generated from the weighted average of 8 component curves having retardation factors ranging from 1 to 500. The composite curve successfully described the observed breakthrough when 25% of the material was very strongly adsorbed (R = 200 and 500), 45% was moderately adsorbed (R = 50 and 100), and 30% was weakly adsorbed (R = 1–10). This distribution agrees at least qualitatively with the adsorption characterization by Rittmann et al. (1992).

In summary, the biotic fate of polydisperse fraction M_w 16,700 was correctly described when a wide range of retardation factors was explicitly made part of the modeling. Although the model's generalizability is limited by the need for several assumptions, it provides an intuitive explanation for the way in which adsorption and biodegradation interact for a polydisperse substrate. In situations like this fate study, in which active biomass already is present from utilization of a primary substrate (glucose here), equilibrium adsorption increases the time to breakthrough and reduces the exiting concentration. Thus, the increase in substrate contact time appears to enhance biodegradation.

Acknowledgements

This research was funded by the Procter & Gamble Co. Special thanks go to Larry W. King for providing materials and valuable technical advice.

References

Chang HT & Rittmann BE (1988) Comparative study of biofilm kinetics on different adsorptive media. *J. Water Pollution Control Federation*, 60: 362–368

Freeze RA & Cherry JA (1979) *Groundwater*. Prentice-Hall Publ., Inc. Engelwood Cliffs, New Jersey

Henry B (1990). Effects of polydisperse size distribution on the simultaneous transport, adsorption, and biodegradation of polyacrylate in a porous medium. M.S. Thesis, Dept. of Civil Engr., University of Illinois, Urbana, IL

Kobayashi H & Rittmann BE (1982) Microbial removal of hazardous organic chemicals. *Environ. Sci. Technol.*, 16: 170A181A

Levenspiel O (1972) Chemical Reaction Engineering, John Wiley & Sons, Inc., New York

McQuarrie KTB, Sudicky EA & Frind EO (1990) Simulation of biodegradable organic contaminants in groundwater. 1. Numerical formulation in principle directions. Water Resources Res. 26: 207–233

Odencrantz JE, Bae W, Valocchi AJ & Rittmann BE (1990) Stimulation of biologically active zones (BAZs) in porous media by electron-accepter injection. J. Contam. Hydrol. 6: 37–52

Odencrantz JE, Valocchi AJ & Rittmann BE (1991) Modeling two-dimensional solute transport with different biodegradation kinetics. Proc. Petroleum Hydrocarbons and Organic Chemicals in Ground Water: Prevention, Detection, and Restoration. National Water Well Assn., pp. 355–368

Rittmann BE, Henry B & Sutfin JA (1992) Biodegradation and sorption properties of polydisperse acrylate polymers. Biodegradation (this issue)

Rittmann BE & McCarty PL (1981) Substrate flux into biofilms of any thickness. J. Environ. Engr. (ASCE) 107: 831–849

Wheeler MF (1988) Modeling of highly advective flow problems. In Developments in Water Science, Vol. 1, Modeling Surface and Sub-Surface Flows. Elsevier Publishers, New York

Wheeler MF & Dawson CN (1987) An Operator Splitting Method for Advection-Diffusion-Reaction Problems. Technical Report 87-9, Dept. of Mathematical Sciences, Rice University, Houston, Texas